7th International Conference on Innovation in High Performance Sailing Yachts and Wind Assisted Ships. InnovSail 2026, Gothenburg, Sweden, 3-5 June 2026.

Life Cycle Assessment and Artificial Intelligence in Wind-Assisted Ship Propulsion

Dilan Hitesh Vaghela*
Birmingham City University, UK.

Minahil Farhan*
Birmingham City University, UK.

Andrew Trujillo
Birmingham City University, UK.

Jean-Baptiste R. G. Souppez
Birmingham City University, UK, jb.souppez@bcu.ac.uk.

*co-first author.

Abstract. Wind-assisted ship propulsion, also referred to as wind power for ships, has established itself as a proven technological solution to reduce shipping emissions and meet increasingly stringent regulations, such as those of the International Maritime Organisation. Indeed, reductions in carbon dioxide emissions have been evidenced for both retrofits and new builds, with increased efficiency achieved thanks to operational optimisation, e.g. weather routing. With numerous options available, ranging from sails to Flettner rotors to kites, and increasing uptake on large vessels, a strong case for wind as both a short and long-term solution can be made. However, there remain limitations in the tank-to-wake approach to life cycle assessment for wind-assisted ships, and recent advances in artificial intelligence afford new opportunities to quantify the emission reduction potential of wind propulsion systems, as well as their commercial viability. Consequently, in this work, we investigate (i) life cycle assessment for wind-assisted ships; (ii) the commercial viability of Flettner rotors in order to identify any optimum cost-effective solution for decarbonization, and (iii) the role of artificial intelligence in advancing and supporting the growth and techno-economic optimization of wind power for ships. These results offer novel insights into recent advances in wind power for ships, particularly with respect to well-to-wake life cycle assessment and the commercial implications of wind propulsion systems for emission reduction through the emerging use of artificial intelligence. It is anticipated that these findings will support future regulatory and policy developments, as well as inform subsequent research directions for maritime decarbonization.

Keywords: wind power for ships, maritime decarbonization, well-to-wake, tank-to-wake, AI.

NOMENCLATURE

$C_{basline}$	Baseline annual CO_2 emissions without wind assistance [tCO_2/year]
C_c	Emissions credit generated by biomass growth [gCO_{2eq}/g]
C_{ccs}	Carbon capture and storage emissions [gCO_2/MJ]
C_{ccu}	Emission credits from used captured CO_2 [gCO_{2eq}/g]
C_{fecu}	Extraction emissions [gCO_2/MJ]
C_l	Carbon stock changes emissions [gCO_2/MJ]
C_{occs}	Emission credits from carbon capture [gCO_{2eq}/g]
C_p	Feedstock processing emissions [gCO_2/MJ]
C_{td}	Feedstock transport emissions [gCO_2/MJ]
C_{saved}	Annual CO_2 emissions reduction due to Flettner rotors [tCO_2/year]

C_{sca}	Soil carbon accumulation [gCO2/MJ]
E	Power [kW]
$f_{basline}$	Baseline annual fuel consumption without wind assistance [t/year]
f_{saved}	Annual fuel savings due to Flettner rotor assistance [t/year]
f_{voy}	Fuel consumption per voyage [t]
G_{WtT}	Greenhouse gas – Well to Tank [gCO_{2eq}/MJ]
G_{TtW}	Greenhouse gas – Tank to Wake [gCO_{2eq}/MJ]
I_0	Initial capital investment [USD]
J_{EOL}	End of life of Flettner Rotor [$kgCO_{2eq}$]
J_i	Installation of Flettner Rotor [$kgCO_{2eq}$]
J_m	Manufacturing of Flettner Rotor [$kgCO_{2eq}$]
J_t	Transportation of Flettner Rotor [$kgCO_{2eq}$]
J_{VOY}	Vessel voyage for Flettner Rotor [$kgCO_{2eq}$]
N	Number of Monte Carlo simulations [-]
P	Fuel saving fraction [-]
Q_{fCH_4}	CH_4 emission conversion factors [gCH_4/g]
Q_{fCO_2}	CO_2 emission conversion factors [gCO_2/g]
Q_{fN_20}	N_2O emission conversion factors [gN_2O/g]
Q_{fug}	Fuel system losses [%]
Q_{sfx}	Fuel GHG content [g GHG/g]
Q_{slip_ship}	Unoxidized fuel slip [%]
r	Discount rate [-]
T	Project lifetime [yr]
t_{voy}	Voyage duration [h]
W_{fuelx}	Global Warming potential of fuel [gCO_{2eq}/g]
W_{CH_4}	Global Warming potential of CH_4 [gCO_{2eq}/g]
W_{CO_2}	Global Warming potential of CO_2 [gCO_{2eq}/g]
W_{N_2O}	Global Warming potential of N_2O [gCO_{2eq}/g]
X_{FR}	Cradle to grave emissions [$kgCO_{2eq}$]

γ_{Fc}	Carbon source factor [-]
γ_{Fccu}	Carbon capture and utilisation factor [USD]
λ_T	Salvage value at project lifetime T [USD]
μ	Net cashflow in year y [USD]
π_0	Carbon penalty at year 0 [USD]
π_{EoL}	End-of-life carbon penalty [USD]
π_y	Carbon penalty in year y [USD]
σ	Net Present Value [USD]
σ_{ECO}	Eco-Net Present Value [USD]

AI	Artificial Intelligence
BSFC	Brake Specific Fuel Consumption
CAPEX	Capital Expenditure
CF	Cashflow
DPP	Discounted Payback Period
EU ETS	European union emissions trading system
GHG	Greenhouse gas
GWP	Global warming potential
HFO	Heavy fuel oil
IPCC	Intergovernmental Panel on Climate Change
ISO	International Organisation of Standardisation
LCA	Life cycle assessment

MAE	Mean absolute error
MAPE	Mean absolute percentage error
MC	Monte Carlo
MCR	Maximum continuous rating
ML	Machine learning
NPV	Net present value
OPEX	Operational expenditure
RF	Random forest
RMSE	Root mean square error
SARIMA	Seasonal autoregressive integrated moving average
SPB	Simple payback period
TtW	Tank-to-wake
WtT	Well-to-tank
WtW	Well-to-wake

1. INTRODUCTION

Shipping accounts for between 80% and 90% of global trade and is responsible for circa 2.5% to 3% of greenhouse gas (GHG) emissions (Dhainaut et al., 2025; Khan et al., 2021). With increasingly more stringent emission regulations (IMO, 2025), primarily driven by the International Maritime Organisation (IMO), wind-assisted ship propulsion (WASP), also referred to as wind power for ships, has emerged as an effective solution to reduce shipping emissions. Indeed, reviews by Bouman et al (2017), Fadaie et al. (2025) and Huang & Souppez (2025) have demonstrated the potential of WASP to reduce CO_2 emissions up to 50%, with the latter quantifying the interquartile benefits of WASP between 7.5% and 22.5% for all technologies (e.g. sails, rotors, kites).

However, the current regulatory boundaries of life cycle assessments (LCA), namely tank-to-wake (TtW) (i.e. fuel burn on the ship) have been increasingly criticised, with a well-to-tank (WtT) approach favoured to ensure accurate quantification of emissions (Ha et al., 2023; Kramel et al., 2021; Roux et al., 2024; Zamboni et al., 2024). This is particularly relevant to sustainable fuels, although the LCA of wind propulsion systems (WPS) remains comparatively under studied.

Moreover, the advent of machine learning and artificial intelligence now offers new opportunities for maritime decarbonization (Nguyen et al., 2025), including for WASP (Lan et al., 2025; Li et al., 2025). Indeed, while cost-benefit analyses are based on constant or short-term average prices (Reche-Vilanova et al., 2025), this does not allow to address long term uncertainty, as fuel savings are the primary factor that determines the economic viability of WASP. Recent developments in machine learning (ML) and artificial intelligence (AI) provide new opportunities to improve long-term price forecasting and risk modelling.

Consequently, this paper explores the application of life cycle assessment and artificial intelligence to wind assisted ship propulsion to identify to which extent WASP contributes to emission reduction in both WtW and TtW LCAs, and the ability of AI to estimate the environmental and economic viability of WASP given long term fuel price uncertainty through an AI-assisted techno-economic framework. The latter is achieved thanks to time-series models (e.g. SARIMA), alongside ensemble learning approaches (e.g. Random Forest regression) to allow future price trajectories to be estimated using historical patterns. By integrating these within a Monte Carlo framework, probabilistic evaluation of investment outcomes is achieved, rather than relying solely on deterministic scenarios.

The remainder of this paper is structured as follows. Section 2 details the methodology and case study employed in this work. Section 3 presents the results for both LCA and application of AI. Finally, the novel findings of this work are summarised in Section 4.

2. METHODOLOGY

This section presents the details of the case study employed in this paper (Section 2.1) and methodology associated with the life cycle assessment (Section 2.2) and the artificial intelligence techno-economic analysis (Section 2.3).

2.1 Case Study

An Ultra Large Container Ship (ULCS), namely the *Evergreen Ever Ace,* fitted with a WinGD X92B engine, was selected as a case study for the purpose of this investigation, with the main specifications listed in Table 1. Here we assume a Shanghai Rotterdam trade route. The one-way sailing distance of 13,815.5 nautical miles was obtained from SeaRates and Oceanlook (SeaRates, 2026; Oceanlook, n.d.), at a service speed of 14 kn. A total of 11 port calls per leg were assumed, see Figure 1, with a median port stay of 23.5 hours per port (UNCTAD, 2023), giving 7 voyages per year, or 6908 h/year at sea, and 1810 h/year of port time. These values are used to annualise fuel consumption and emissions in the analysis.

Table 1. Evergreen Ever Ace specification (Evergreen, 2021)

Capacity	23,992 TEU
Length overall	399.9 m
Beam	61.5 m
Draft	~17 m
Deadweight tonnage (DWT)	~241,000 tonnes
Service speed (operational)	14 knots

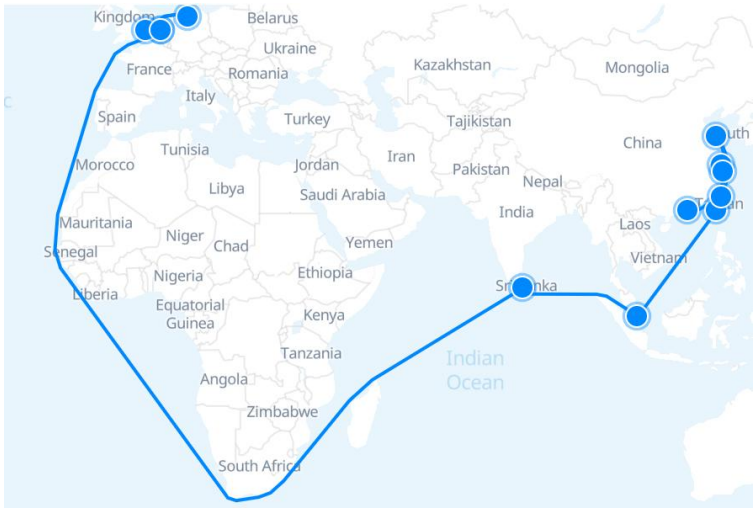

Figure *1.* *Evergreen Ever Ace voyage route (SeaRates, 2026).*

The WPS selected for this investigation is a Flettner rotor, shown by Huang and Souppez (2025) to yield the greatest carbon dioxide (CO_2) emissions reduction potential based on a systematic review of the WASP literature. However, the emissions from methane (CH_4) and nitrous oxide (N_2O) have been accounted for as both the gases have a higher global warming potential based on the Intergovernmental Panel on Climate Change (IPCC) equivalent CO_2 conversions (Ipcc.ch, 2023). The IPCC conversions allow for other gas emissions to be converted to CO_2 emissions. Here, we base the Flettner rotor on that of Kim et al. (2024), depicted in Figure 2, for which masses and materials are detailed in Table 2, with components either made of glass-fibre reinforced polymer (GFRP) composite or steel. Each of the three rotors considered in this work is 30 m tall by 3 m diameter.

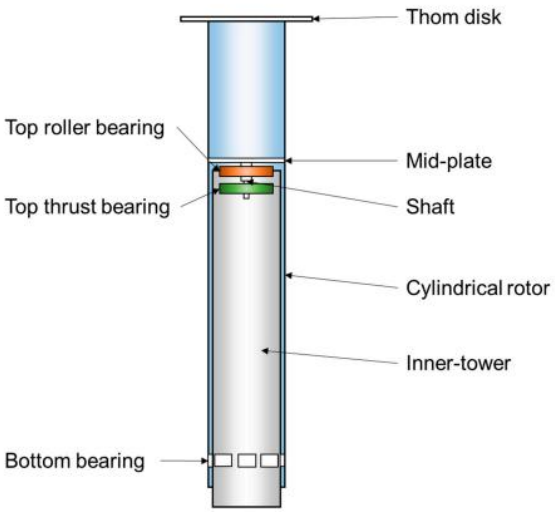

Figure 2. Flettner rotor components, reproduced from Kim et al. (2024).

Table 2. Mass and material of Flettner rotor subcomponents (Kim et al., 2024).

Components	Mass [kg]	Material
Thom disk	1096.9	GFRP Composite
Mid-plate	6689	Structural Steel
Shaft	1692.7	Structural Steel
Cylindrical Rotor	8530.3	GFRP Composite
Inner Tower	49678	Structural Steel

Four scenarios will be considered in this work, a baseline case without Flettner rotor, and a low (scenario a), medium (scenario b) and high (scenario c) case for the benefits of Flettner rotors, respectively quantified as a 10.5%, 18% and 28.5% emissions reduction potential. These numbers correspond to the lower quartile, median and upper quartile according to the systematic review of Huang & Souppez (2025). The annual fuel and CO_2 savings are defined as proportional reductions relative to the baseline operational emissions:

$$f_{\text{saved}} = f_{\text{baseline}}\, P \tag{1}$$

$$C_{\text{saved}} = C_{\text{baseline}}\, P \tag{2}$$

Equations (1) and (2) calculate the annual fuel savings and CO_2 emissions reductions by applying the fractional reduction P which represents the fractional emissions reduction (0.105, 0.18 and 0.285 for the low, medium and high benefit case, respectively) from Flettner rotor assistance to the baseline fuel consumption and baseline CO_2 emissions of the vessel. These reduction fractions are applied consistently throughout the life-cycle assessment, technical and economic phases of the study.

Fuel and carbon prices are based on the January 2019-February 2026 period for the former, and European Union (EU) Emissions Trading System (ETS) for the latter and are represented using percentile-based scenarios to avoid reliance on a single assumed market condition and to reflect historical volatility (Reche-Vilanova et al., 2025). In this context, the 25th, 50th and 75th percentiles (P25, P50 and P75) of the historical price distributions are used to represent low, median and high market conditions, respectively. These percentile values define the fuel and carbon price levels used in the deterministic economic analysis and are given in Table 3.

Table 3. Assumed fuel (Bunker, 2019) and carbon (Investing.com UK, 2023) prices

Market condition	Fuel price [USD/t fuel]	Carbon price [USD/tCO2]
Low (25th percentile)	405	61
Median (50th percentile)	480	79
High (75th percentile)	523	91

In contrast, Phase 3 simulation outcomes are summarised using Monte Carlo percentile indicators (P10, P50 and P90), representing the 10th, 50th and 90th percentiles of the simulated result distributions. These indicators provide a wider representation of uncertainty and are widely used in financial risk analysis to describe the range and likelihood of possible investment outcomes under uncertain fuel and carbon price trajectories (Glasserman, 2004).

2.2 Life Cycle Assessment

The LCA is undertaken using the OpenLCA (Openlca.org, 2026) software together with the BAFU database (Admin.ch, 2026), which contains processes and flows that allow for LCA modelling with modifiable data. The defined functional unit for this case study is a single 1 nm, with the ship boundaries including production and supply of heavy fuel oil (HFO) for WtT, as well as combustion and direct exhaust for TtW. The cradle-to-grave model adopted for the Flettner rotor considers manufacturing, transportation from China (Anemoi, 2024), installation, and maintenance. Both approaches are depicted in Figures 3(a) and 3(b), respectively.

Well-to-wake life cycle assessment is undertaken following the IMO regulation (IMO, 2023) for GHG of marine fuels, with well-to-tank emissions given as

$$\mathrm{G}_{WtT} = C_{fecu} + C_l + C_p + C_{td} - C_{sca} - C_{ccs}, \tag{3}$$

where C_{fecu} is the emissions associated with extraction, C_l is the emissions from carbon stock exchanges, C_p is the processing emissions during conversion of feedstock to the final fuel product, C_{td} is the emissions from transportation of the feedstock, C_{sca} is the soil carbon accumulated emissions and C_{ccs} is emissions credit from carbon capture and storage that has not been accounted for in C_p.

Additionally, the tank-to-wake emissions are computed as

$$\mathrm{G}_{TtW} = \frac{1}{L}\left[\begin{array}{l}\left(1 - \frac{1}{100}\left(Q_{slip\_ship} + Q_{fug}\right)\right) \times \left(Q_{fCO_2} + \mathrm{W}_{CO_2} + Q_{fCH_4} \times \mathrm{W}_{CH_4} + Q_{fN_20} \times \mathrm{W}_{N_2O}\right) \\ + \left(\frac{1}{100}\left(Q_{slip\_ship} + Q_{fug}\right) \times Q_{sfx} \times \mathrm{W}_{fuelx}\right) - \gamma_{Fc} \times C_c - \gamma_{Fccu} \times C_{ccu} - C_{occs}\end{array}\right], \tag{4}$$

where L is the low calorific value of the fuel used, $Q_{slip_{ship}}$ is the percentage of total fuel mass, Q_{fug} is a percentage of mass fuel escaping between the tanks, Q_{slip} is percentage of total fuel mass which escapes from the energy convertor without being oxidized, Q_{sfx} is the share of GHG in the components of fuel, Q_{fx} are the emission conversion factors for the GHG as x represents the gasses (CO_2, CH_4, N_2O), γ_{FC} is the carbon source factor, C_c are the emissions credit and with the other components representing specific scenarios. Results are generated for the Global Warming Potential for 20 years (GWP20), employing IPCC CO_2 emission conversions.

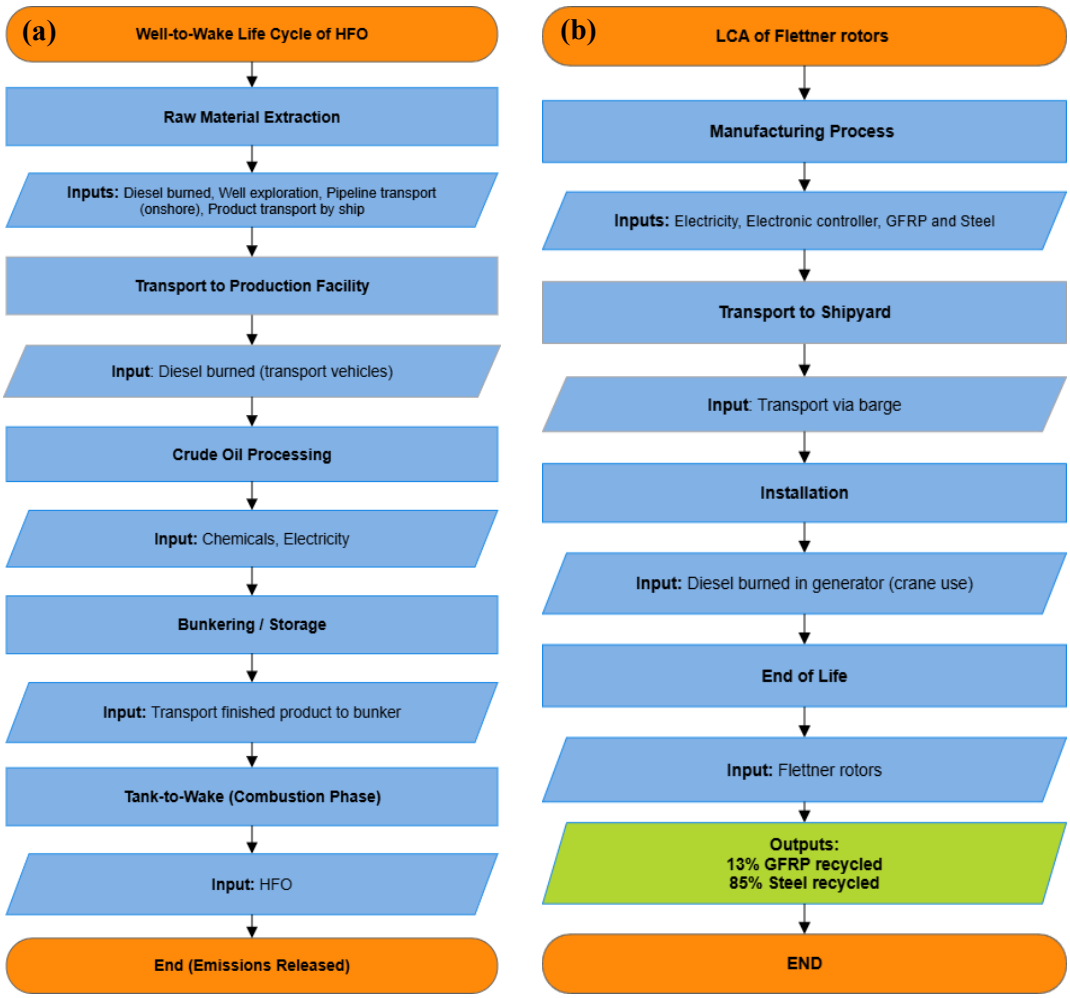

Figure 3. LCA methodology for (a) the well-to-wake ship emissions, and (b) for Flettner Rotor.

The LCA modelling for the 3 Flettner rotors, X_{FR}, is computed as

$$X_{\mathrm{FR}} = J_m + J_t + J_i + J_{Voy} + J_{EOL}. \tag{5}$$

The method includes the following considerations and assumptions:

- manufacturing, J_m, assuming 1.0522×10^5 kWh of electricity, 28.9t of GFRP, 174.2 t of steel, and 900 kg of electrical units (Kim et al. 2024; Marketreportsworld.com. 2026);
- transportation, J_t, and installation, J_i, considers the tugboat engine power as 3482 kW, distance transported as 300 km and the crane's generator as 50 W (Chen and Lam, 2022; Tillig et al., 2020);
- voyage savings, J_{VOY}, considering maintenance at 2.21×10^{-5} per nm and allocation for the rotors at 4.136×10^{-7} per nm. The fuel used through the voyage is 422.96 kg/nm with a Brake Specific Fuel Consumption (BSFC) of 154.3 g/kWh. The allocation is based on calculations made from the lifetime years of the rotor, voyages per year and the nautical miles per voyage; and
- J_{EOL}, which considers the recycling of the Flettner rotor components, with recycling rates of 85% for steel and 13% for GFRP based on Watari et al. (2025) and Karuppannan Gopalraj and Kärki (2020).

The Flettner rotors will be powered by the ship's auxiliary engines as included explicitly in the LCA (Arabnejad et al., 2025), as well as maintenance has been allocated as a once-a-year event (Anemoi, 2024).

2.3 AI-Assisted Techno-Economic Framework

Here, we assess the vessel's yearly operational performance over a 25-year economic lifetime, with an AI methodology divided into three phases: Phase 1 which tackles performance prediction, Phase 2 which covers the economic model, and Phase 3 which considers long-term forecasting and uncertainty. These processes are depicted in Figures 4(a), 4(b) and 4(c), respectively.

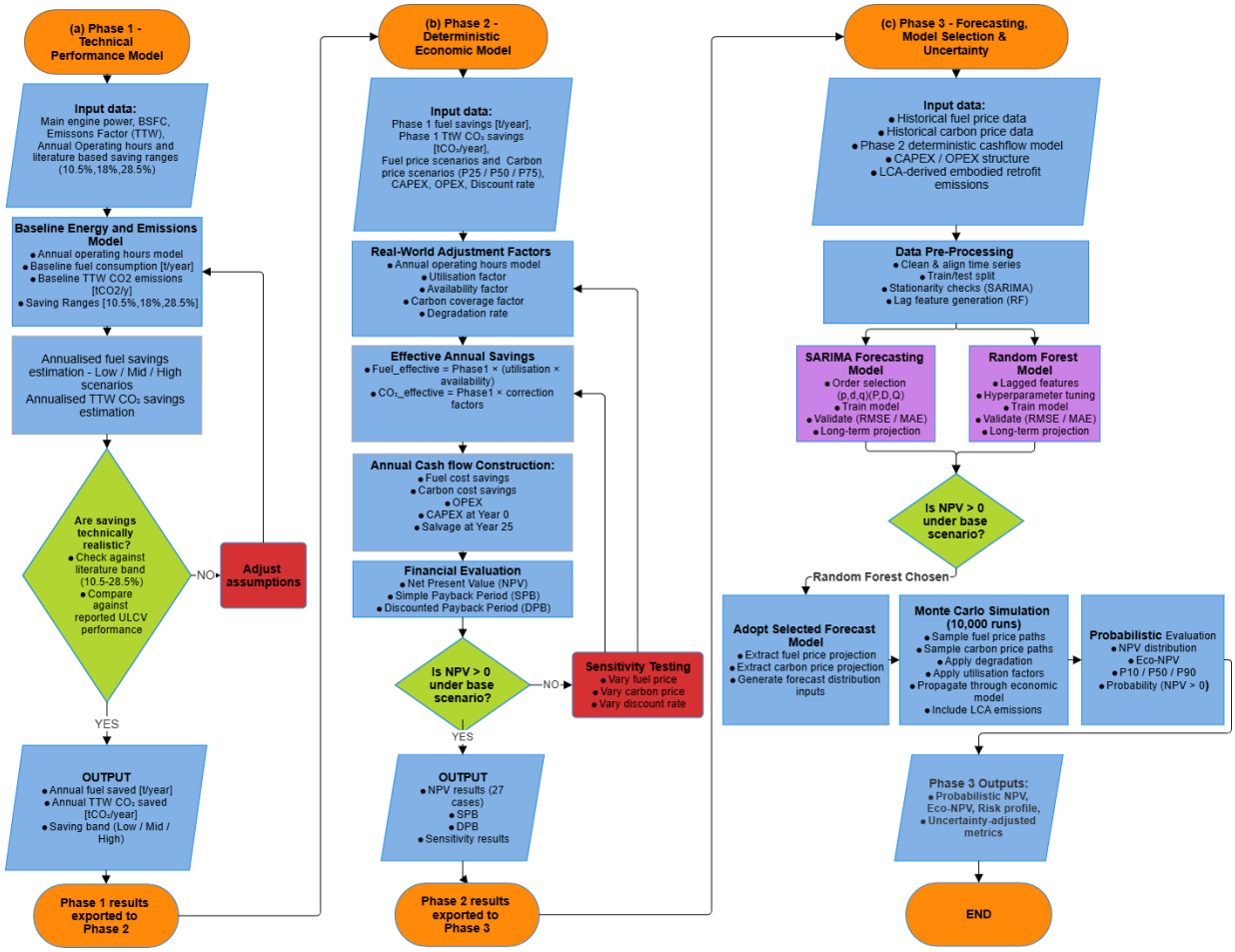

Figure 4. AI-Assisted Techno-Economic Framework for (a) phase 1; (b) phase 2 and (c) phase 3.

2.3.1 Phase 1: Performance Modelling

In this first phase, baseline annual fuel consumption and Tank-to-Wake CO_2 emissions are first calculated using engine and operating data, as defined in Section 2.1. From the LCA's functional unit, voyage-level fuel consumption and emissions are scaled to support the 25-year techno-economic assessment. Using an effective propulsion power of 38,362.5 kW, a BSFC of 154.36 g/kWh, an emission factor of 3.114 gCO_2/g fuel, and 6,908 annual open-sea operating hours, the baseline performance was calculated as 40,904 t/year of fuel consumption and 127,376 tCO_2/year of TtW emissions.

The emissions reduction parameter P is applied to the baseline fuel consumption and TtW CO_2 emissions to estimate the savings from wind-assisted ship propulsion. These calculated fuel and emissions reductions are used as inputs for the Phase 2 economic analysis and for integrating operational TtW reductions into the 25-year life-cycle assessment.

2.3.2 Phase 2: Deterministic Economic Model

Phase 2 converts the Phase 1 annual fuel and TtW CO_2 savings into a deterministic investment business case using a discounted cashflow model over a 25-year lifetime (Reche-Vilanova, 2025). The model evaluates the economic viability of a three-unit rotor sail retrofit on Ever Ace by combining capital expenditure (CAPEX), additional operational costs (OPEX), and realised fuel and carbon savings under different market scenarios. To move from ideal technical savings to economically realised savings, a set of operational and regulatory adjustments are applied. These adjustments reflect real-world implementation conditions rather than theoretical performance, and are applied to the Phase 1 savings before financial evaluation:

1) utilisation factor: rotors are not effective all the time because wind conditions vary (Norsepower, 2022);
2) availability factor: allowance for downtime, maintenance, and operational interruptions (Carlton, 2018);
3) carbon coverage factor reflects that not all CO_2 savings are exposed to carbon pricing for example partial European Union Emissions Trading System (EU ETS) route coverage; and
4) performance degradation: performance is assumed to reduce slightly each year over the lifetime (Hamilton et al., 2020).

These factors convert idealised annual savings into effective annual economic savings. This approach aligns with implementation-oriented wind propulsion cost-benefit structures that incorporate operational penalties when transitioning from physics-based savings to business-case modelling (Reche-Vilanova, 2025). Fuel and CO_2 savings remain proportional under TtW accounting to ensure consistency between the technical and economic models (Huang & Souppez, 2025). The key economic and operational assumptions applied in Phase 2 are summarised in Table 4.

Table 4. Key techno-economic model parameters used in the discounted cash flow and Monte Carlo analysis.

Parameter	Value	Purpose
Project lifetime	25 years	Ship lifetime
Discount rate range	3%, 7%, 10%	Sensitivity testing of financial performance
Utilisation factor	0.35	Fraction of time favourable wind conditions
Availability factor	0.95	Technical uptime allowance for rotor system operation
Carbon coverage	0.50	Fraction of CO_2 savings exposed to carbon pricing
Degradation rate	0.5% per year	Long-term decline in technology performance
CAPEX	6,000,000 USD	Estimated retrofit investment for three rotor sails
Salvage value	15% of CAPEX at end-of-life	Residual value recovered at end of asset life
Maintenance cost	2% of CAPEX per year	Additional operational expenditure
Electrical demand	650,000 kWh/year	Auxiliary electricity consumption
Electricity price	0.12 USD/kWh	Industrial electricity cost assumption
Survey & certification cost	60,000 USD/year	Annual classification inspection, certification and operational compliance costs

For the cashflow construction, annual gross savings are calculated from realised fuel savings and the portion of CO_2 savings exposed to carbon pricing under the fuel and carbon price scenarios, with savings declining gradually over time due to the degradation factor. Net annual cashflow is obtained by subtracting additional operating expenditures associated with the rotor sail system from annual

savings. These expenditures include maintenance costs, auxiliary electricity consumption, and annual survey and certification costs. To reflect market uncertainty, sensitivity tests are also conducted by varying fuel price, carbon price, and discount rate.

Economic feasibility is evaluated using three standard financial indicators: Net Present Value (NPV), given as σ in Equation 6; Simple Payback Period (SPB), which represents the time required for cumulative net cashflows to recover the initial investment; and discounted Payback Period (DPP), that accounts for the time value of money by using discounted cashflows.

$$\boldsymbol{\sigma = -I_0 + \sum_{y=1}^{T} \frac{\mu}{(1+r)^y} + \frac{\lambda_T}{(1+r)^T}} \quad (6)$$

where I_0 is the initial capital investment (CAPEX) at year 0, μ is the net annual cashflow in year y, r denotes the discount rate, which accounts for the time value of money, T represents the total project lifetime, and λ_t corresponds to the residual (salvage) value recovered at the end of the project lifetime.

The discounted cash flow structure, degradation modelling, and operational adjustment methodology are consistent with established engineering economic theory (Blank & Tarquin, 2018; Fisher, 1930) and with wind propulsion techno-economic frameworks reported by Reche-Vilanova (2025). The proportional relationship between fuel and TtW CO_2 reduction follows the synthesis approach described by Huang & Souppez (2025) and established IMO carbon accounting practice.
Phase 2 therefore establishes a structured and reproducible deterministic economic baseline linking technical performance to investment feasibility over a 25-year horizon. However, fuel and carbon prices exhibit long-term volatility and structural uncertainty that cannot be captured through fixed percentile scenarios alone. Consequently, Phase 3 extends this framework through AI/ML-based forecasting and Monte Carlo simulation to quantify price uncertainty and evaluate investment robustness under stochastic market conditions.

2.3.3 Phase 3: AI/ML and Uncertainty Model

Phase 3 continues the deterministic economic model developed in Phase 2 by introducing uncertainty in long-term fuel and carbon prices. Instead of fixed price scenarios, forecasting models are used to produce stochastic price trajectories which are propagated through a Monte Carlo simulation. This enables the economic and environmental performance of wind-assisted ship propulsion to be evaluated under realistic market volatility while maintaining the same 25-year lifetime and the three scenarios (low, medium, high savings).

Historical fuel and carbon price data described in Section 2.1 were used as inputs to the forecasting framework. A statistical time-series model and a machine-learning model were implemented for comparison and validation. A Seasonal Autoregressive Integrated Moving Average (SARIMA) model was used as a transparent statistical benchmark capable of representing trend and seasonal behaviour commonly observed in energy price series (Box et al., 2015; Hyndman & Athanasopoulos, 2021). In comparison, a Random Forest regression model was applied to capture nonlinear relationships in the price series using lagged variables and rolling statistical features (Breiman, 2001; Pedregosa et al., 2011). Together these models form an AI-assisted forecasting framework, combining traditional statistical modelling with machine-learning techniques.

Validated forecasts are then integrated into the techno-economic model using a Monte Carlo simulation implemented in MATLAB with 10,000 runs. Fuel prices, carbon prices and selected operational parameters were sampled within realistic ranges, and annual cashflows were calculated using the cost structure defined in Phase 2.

Lifecycle emissions were integrated into the Monte Carlo model using the LCA results described in Section 2.2. Fixed lifecycle emissions from manufacturing, installation, and end-of-life of the rotor system were included. These emissions were monetised using the simulated carbon price and incorporated into the economic model through the Eco-NPV metric, which extends the standard NPV by accounting for carbon costs during installation, operation, and end-of-life. This is computed as

$$\boldsymbol{\sigma_{\mathbf{ECO}}} = -I_0 - \pi_0 + \sum_{y=1}^{T} \frac{\mu - \pi_{\mathrm{y}}}{(1+r)^y} + \frac{\lambda_T - \pi_{\mathrm{EoL}}}{(1+r)^T} \tag{7}$$

where σ_{ECO} is the Eco-Net Present Value (Eco-NPV), I_0 is the initial investment cost, π_0 is the carbon penalty in year 0, μ is the annual net cash flow, π_y is the carbon penalty in year y, r is discount rate is, T is the project lifetime, λ_T is the salvage value at year T , and π_{EoL} is the end-of-life carbon penalty.

The economic model assumes a 25-year vessel lifetime, which reflects the typical service life of large commercial ships and retrofit investments. However, the LCA results use the IPCC and global warming potential (GWP20), which evaluates climate impacts over a 20-year period. Therefore, the end-of-life emissions from the LCA are applied in Year 20 to remain consistent with the available dataset. Since these emissions occur only once and are discounted in the financial model, applying them in Year 20 instead of Year 25 has very little impact on the Eco-NPV results. Monte Carlo simulation results are summarised using P10, P50 and P90 percentiles, representing optimistic, median and conservative outcomes.

This forecasting and uncertainty framework follows established financial risk modelling approaches where uncertain inputs are propagated through discounted cash-flow models to evaluate investment risk (Glasserman, 2004; Kroese et al., 2011). By combining statistical forecasting, machine-learning models and Monte Carlo simulation within the techno-economic structure developed in earlier phases, Phase 3 provides an AI-assisted techno-economic uncertainty analysis of wind-assisted ship propulsion performance. Before the forecasts are used for long-term price trajectories; the forecasting models must first be validated and compared to determine which approach best represents price behaviour

2.3.4 Validation

For Phase 1, the annual baseline fuel consumption and TtW CO_2 emissions were checked for physical consistency using the engine parameters and operating hours defined in Section 2.1. The resulting baseline values and the linear scaling of savings using the reduction factor P follow standard IMO-style carbon accounting practice and ensure that fuel and CO_2 savings remain proportional throughout the study.

For Phase 2, the discounted cashflow model was validated through behavioural checks rather than repeating derivations. Using the assumptions summarised in Table 4, the model responds as expected: higher fuel and carbon prices increase annual savings and improve economic indicators, while higher discount rates reduce NPV and extend payback periods. This trend is consistent with established engineering economy theory and wind propulsion techno-economic frameworks (Blank & Tarquin, 2018; Fisher, 1930; Reche-Vilanova, 2025), supporting the credibility of the deterministic business case before uncertainty is introduced.

For Phase 3, model validation was performed using a time-ordered hold-out approach where the final 12 months of observations were reserved as an out-of-sample test period. This preserves the temporal structure of the data and avoids information leakage, which is essential for financial time-series forecasting (Bergmeir & Benítez, 2012).

Figure 5 presents the validation results for both forecasting models. The SARIMA validation plots are shown in Figure 5(a) and Figure 5(b) for fuel and carbon prices respectively. These plots compare one-step-ahead forecasts with the observed price series during the hold-out period. In both cases the SARIMA forecasts follow the overall direction of the realised data and remain within the 95% prediction bands, indicating that the models provide a reasonable statistical representation of the underlying price dynamics. The Random Forest validation results are presented in Figure 5(c) and Figure 5(d) for the fuel and carbon prices, respectively. Compared with SARIMA, the Random Forest forecasts respond more strongly to short-term changes and nonlinear movements in the data. This behaviour is particularly visible for the fuel price series, where Random Forest better captures the downward trend observed during the hold-out period.

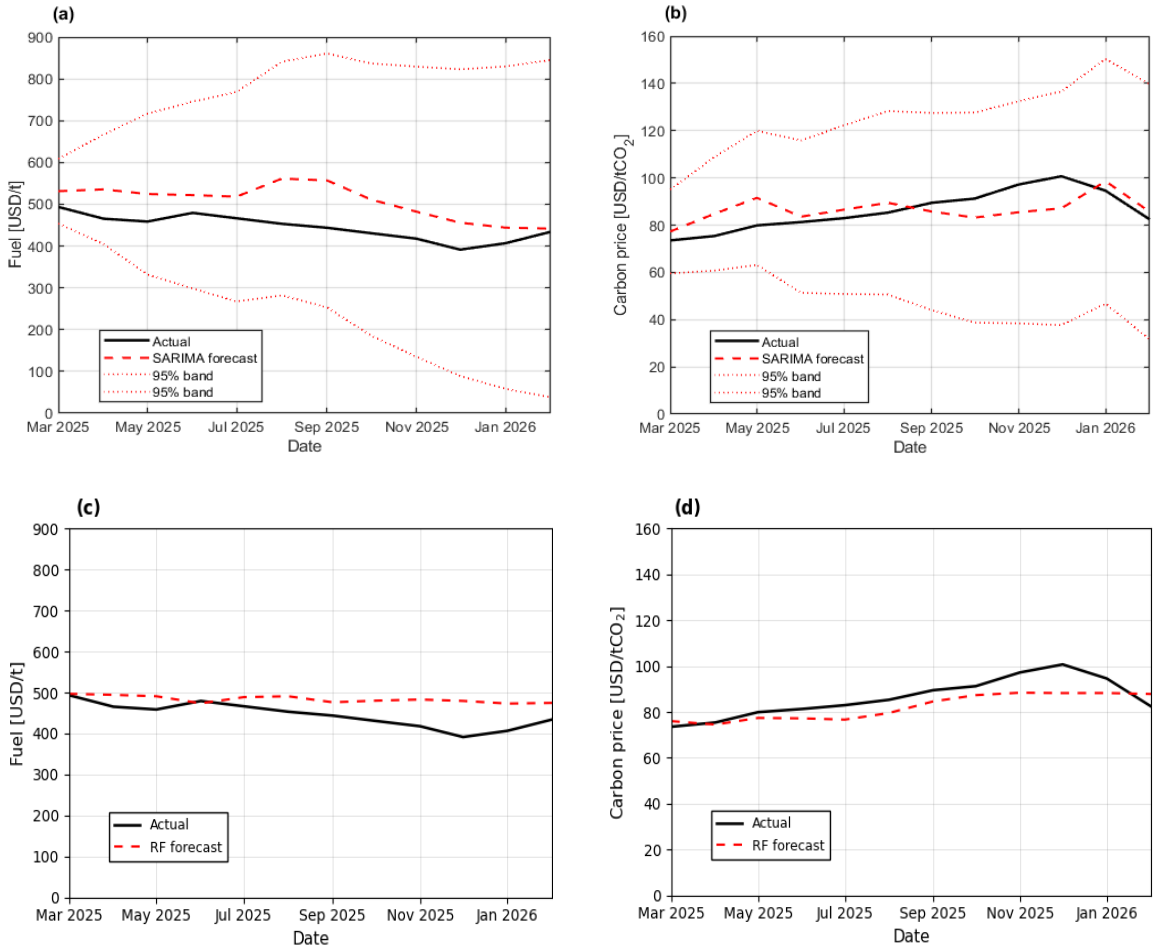

Figure 5. Validation results for (a) fuel and (b) carbon price using SARIMA, and for (c) fuel and (d) carbon price using Random Forest.

Forecast accuracy was evaluated using three standard metrics: Root Mean Square Error (RMSE), Mean Absolute Error (MAE), Mean Absolute Percentage Error (MAPE) and Ljung-Box test is used for the SARIMA model to check whether residuals are independent and contain no remaining autocorrelation. Table 5 summarises the validation results for both forecasting models. The results show that the Random Forest model achieves lower prediction errors for both price series. For fuel prices, Random Forest achieves a MAPE of 9.23% compared with 14% for SARIMA, while for carbon prices the error decreases from 7.57% to 5.96%. These values fall within the range typically considered acceptable for volatile commodity markets such as bunker fuel and carbon allowance prices (Weron, 2014; Zhang et al., 2019).

Table 5. Forecast RMSE, MAE, and MAPE predictive accuracy for SARIMA and Random Forest fuel and carbon price using a 12-month validation period.

Price Series	Model	RMSE	MAE	MAPE	Ljung-Box
Fuel	SARIMA	68.30 USD/t	–	14.0%	0.142
Fuel	Random Forest	46.01 USD/t	39.35 USD/t	9.23%	–
Carbon	SARIMA	7.64 USD/tCO_2	–	7.57%	0.065
Carbon	Random Forest	6.09 USD/tCO_2	5.32 USD/tCO_2	5.96%	–

Given its improved predictive accuracy and better representation of short-term price variability, the Random Forest model is selected to generate stochastic fuel and carbon price trajectories for the Monte Carlo uncertainty analysis. A total of 10,000 simulations were performed to ensure stable probabilistic results (Glasserman, 2004).

3. RESULTS

This Section details the results of the life cycle assessment in Section 3.1, and of the AI-assisted techno-economic framework in Section 3.2, highlighting the novel contributions of this work.

3.1 **Life Cycle Assessment**

Results for GWP20 are presented in Figure 6(a), comparing the Flettner rotor scenarios to the baseline voyage. Whilst the three main GHG variables are CO_2, N_2O and CH_4, the results show negligible levels of N_2O and CH_4. Figure 6(a) further presents the WtT emissions, with Figure 6(b) provides the emissions at other stages of the whole lifecycle assessment.

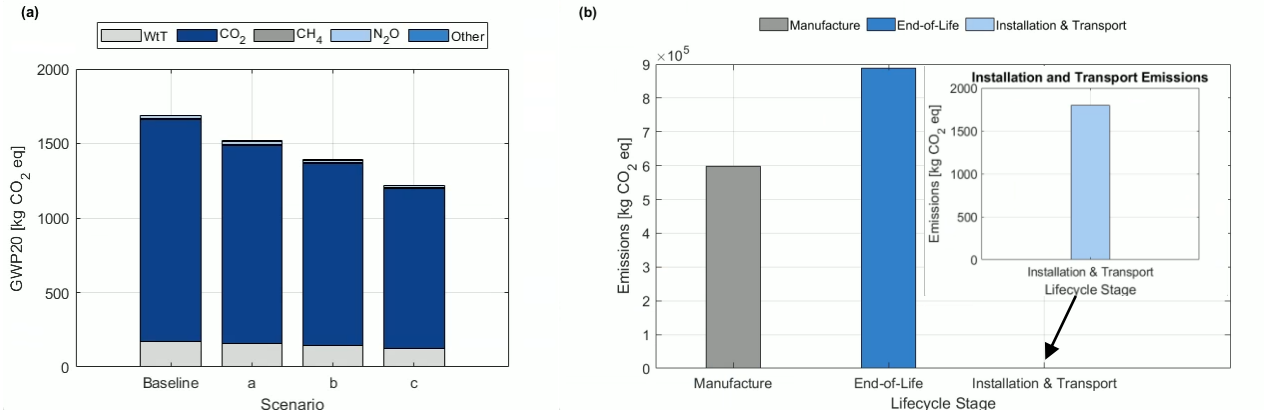

Figure 6. GWP20 emissions for the baseline and Flettner rotor scenarios: (a) well-to-wake emissions and (b) cradle to grave emissions from Flettner rotor manufacture.

The baseline emissions consist of the vessel without Flettner rotors, and leads to the highest GWP 20 at 1515.6 kg CO_2 eq per nm. Scenario a (10.5% savings) yields a GWP 20 of 1360.9 kg CO_2 eq per nm, while scenario b (18% savings) results 1247.2 kg CO_2 eq per nm, and scenario c (28.5% savings) leads to 1087 kg CO_2 eq per nm. These figures are in line with previous fuel saving estimates for Flettner rotors (Hochkirch and Bertram, 2022; Kolodziejski and Sosnowski, 2025).

The WtT emissions show a lower, yet non-negligible, level compared to TtW. For the baseline case, WtT contribute to 11.5% of the total emissions. In terms of the cradle to grave analysis, it indicates that the end-of-life is the highest contributor of emissions, with 8.892×10^5 kg CO_2 for 3 rotors, with manufacturing being the second highest at 5.975×10^5 kg CO_2 for 3 rotors. On the other hand, installation and transportation show a negligible impact on emission levels. The results demonstrate a clear reduction as WASP is introduced, with the Flettner rotors leading to measurable GWP20 reductions, thus, WASP can deliver long term climate benefits. This is further supported by Figure 7, presenting the emissions of the main gases affecting the environment. Despite N_2O, CH_4 and other

gases contributing a small fraction of the total GWP20, N_2O has a GWP 264 times its mass when converted to kg CO_2 eq, while CH_4 has a GWP 84 times its mass. However, even after conversion to CO_2 equivalent, their contribution remains minor compared to CO_2.

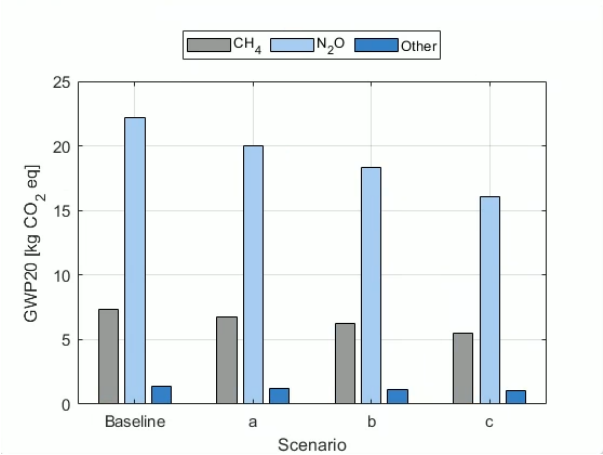

Figure 7. Contribution of minor greenhouse gases to GWP20 emissions for the baseline and rotor-assisted scenarios.

3.2 AI-Assisted Techno-Economic Framework

3.2.1 Phase 1

Phase 1 results are summarised in Table 6 and provide key inputs for Phase 2. Annual fuel savings are converted into fuel cost savings using bunker fuel prices, while CO_2 reductions estimate avoided EU ETS carbon costs, which are used in discounted cash flow calculations for NPV and payback analysis.

Table 6. Annual fuel consumption, fuel savings, and CO_2 emission reductions for the baseline vessel and Flettner rotor performance scenarios.

Scenario	Fuel Consumption [t/year]	Fuel Savings [t/year]	CO_2 Emissions Reduction [tCO_2/year]
Baseline	40,904	–	–
10.5%	36,609.3	4,295.0	13,374.5
18%	33,541.5	7,362.8	22,927.7
28.5%	29,246.6	11,657.7	36,802.1

3.2.2 Phase 2

Figures 8(a) and 8(b) respectively present the simple and discounted payback periods for the Flettner rotor retrofit under market conditions represented by the 25th, 50th and 75th percentiles of historical fuel and carbon prices.

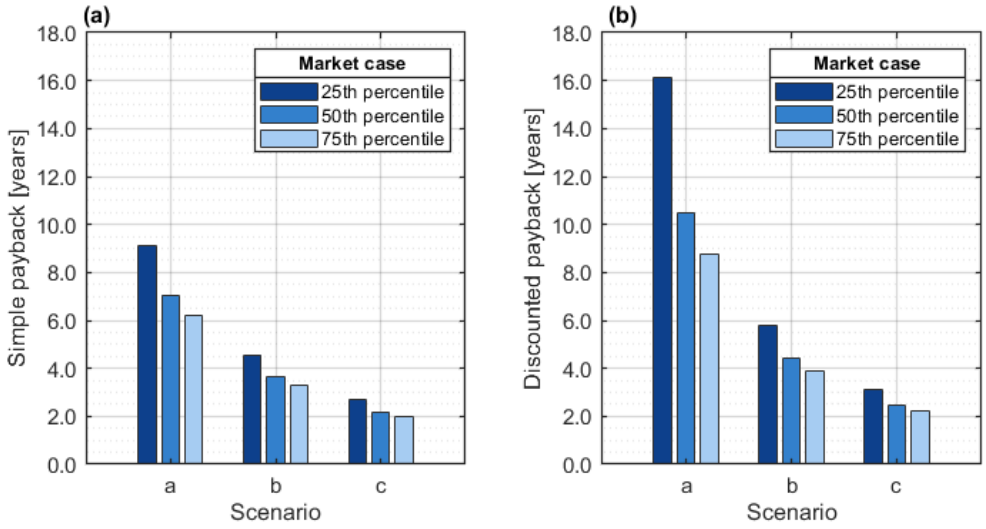

Figure 8. Simple payback period (a) and discounted payback period (b) for the three Flettner rotor performance scenarios under different market fuel price percentiles

Across all cases, payback improves as propulsion savings increase from 10.5% (scenario a) to 28.5% (scenario c). Simple payback ranges from 9.1 to 2.7 years at the 25th percentile, 7.1 to 2.2 years at the 50th percentile, and 6.2 to 2.0 years at the 75th percentile. Discounted payback ranges from 16.1 to 3.1 years, 10.5 to 2.5 years, and 8.7 to 2.2 years, respectively. These results fall within ranges reported in previous wind-assisted ship propulsion studies. For example, Reche-Vilanova (2025) reports payback periods of 3-8 years, while DNV (2021) and Norsepower (2022) indicate that high-performing installations on large vessels can achieve payback within 2-6 years. The close agreement with literature supports the realism of the techno-economic modelling assumptions.

Then, the economic performance of the Flettner rotor retrofit is shown in Figures 9(a). NPV increases significantly as propulsion savings rise from 10.5% to 28.5%, reaching values between approximately 1.3 MUSD and 28 MUSD across the analysed cases. These results highlight the strong financial benefit of fuel savings over the vessel lifetime. Furthermore, Figure 9(b) depicts the cumulative discounted cashflow, where the investment recovers the initial CAPEX after approximately 4.4 years, after which sustained positive economic returns for the remainder of the operating period is generated.

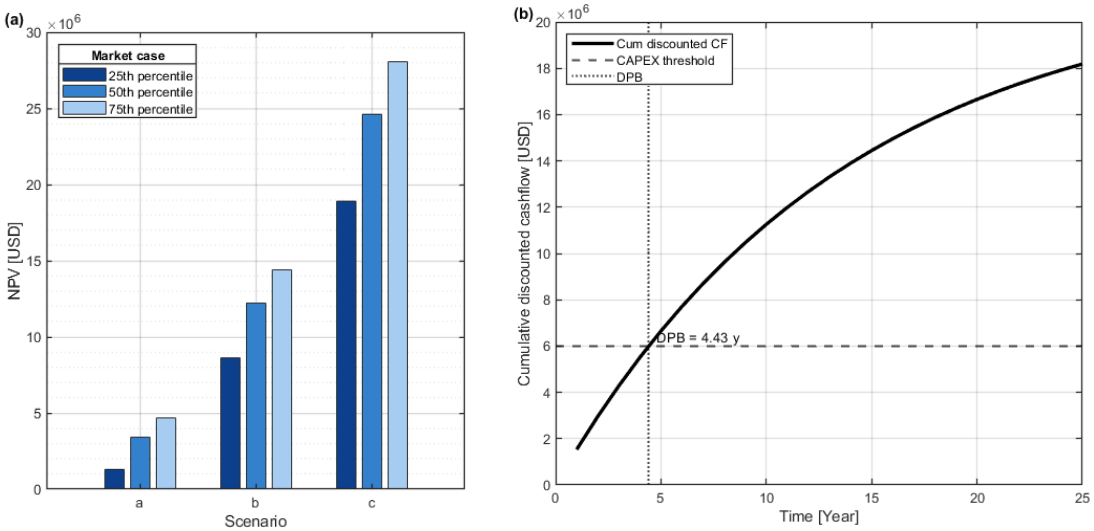

Figure 9. NPV results (a) for the Flettner rotor scenarios under different fuel price cases (P25, P50, P75), and cumulative discounted cashflow (b) showing the discounted payback period.

The economic performance of the Flettner rotor retrofit varies with fuel and carbon price assumptions. For the medium performance case (scenario b, or 18% savings), Figure 10 quantifies the NPV for varying fuel and carbon prices.

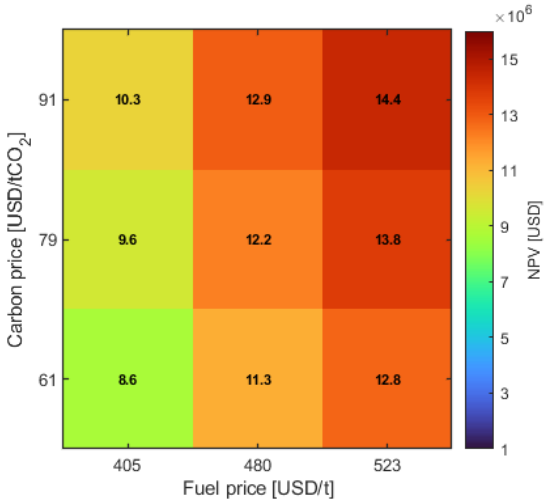

Figure 10. NPV sensitivity to different fuel prices and carbon prices for the 18% fuel-saving scenario.

NPV is shown to increase with both fuel and carbon prices because higher fuel costs increase the value of fuel savings, while higher carbon prices raise the financial benefit of emissions reductions. The resulting NPV range (8-14.4 MUSD) is consistent with values reported for large commercial vessels in previous studies (Reche-Vilanova, 2025; CE Delft, 2016), supporting the validity of the modelling assumptions. However, these deterministic results do not capture the volatility of fuel and carbon markets, which can significantly influence long-term investment outcomes, hence the need for Phase 3

3.2.3 Phase 3

Figure 11 presents the Monte Carlo simulation results for NPV and Eco-NPV across the three Flettner rotor performance scenarios. Each histogram shows the distribution of outcomes from 10,000 simulations, while the vertical lines represent the P10, mean, P50 (median), and P90 percentiles. In the 10.5% case, shown in Figures 11(a) and 11(b), the mean NPV is ~2.5 MUSD, with P10 slightly negative, indicating a small risk of loss but generally positive outcomes. In the 18% scenario, depicted in Figures 11(c) and 11(d), the mean increases to ~10.6 MUSD, with P10 remaining strongly positive, showing robust profitability. Lastly, the 28.5% scenario, presented in Figures 11(e) and 11(f), produces the strongest results, with mean values ~22 MUSD and P10 above 18 MUSD, indicating high financial resilience. Differences between NPV and Eco-NPV are minimal, suggesting lifecycle carbon costs have limited impact on overall investment viability. Overall, the distributions are narrow, indicating stable simulation behaviour with limited extreme outcomes. The small gap between NPV and Eco-NPV shows that including lifecycle carbon costs slightly lowers returns but does not change the overall economic viability of the investment.

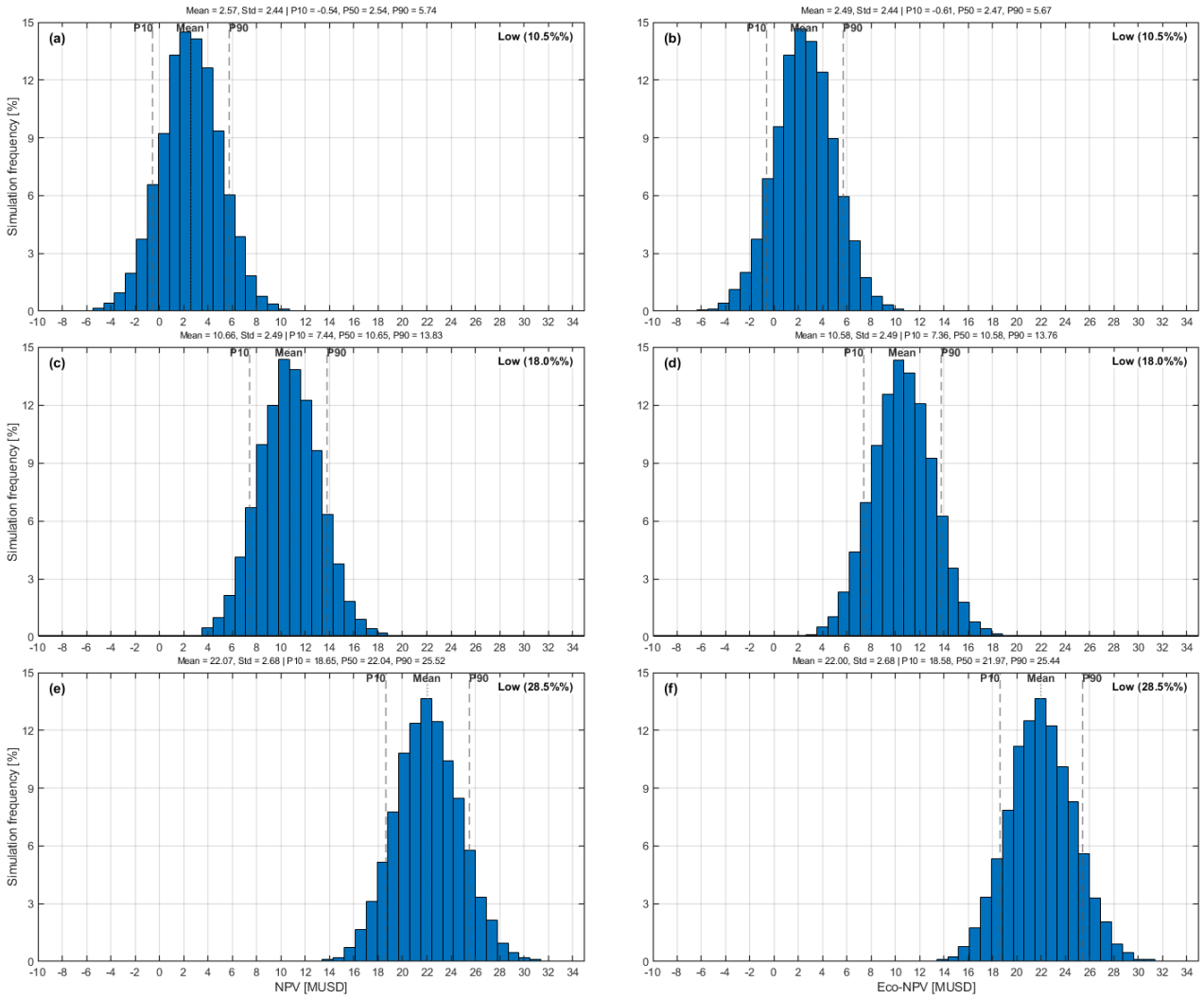

Figure 11. Monte Carlo distributions of NPV (a, c, e) and Eco-NPV (b, d, f) for the 10.5%, 18%, and 28.5% fuel-saving scenarios, showing uncertainty ranges and key percentiles (P10, P50, mean, P90).

Figure 12 presents the uncertainty ranges for the SPB and DPP derived from the Monte Carlo simulations across the three fuel-saving scenarios. The markers represent the median values (P50), while the error bars show the P10-P90 uncertainty ranges. In the 10.5% savings scenario, the median SPB is ~8 years, while the DPP increases to 11-12 years because of discounting future cash flows. The uncertainty range is wider in this case, reflecting the greater sensitivity of the investment to fuel and carbon price variability under lower performance assumptions.

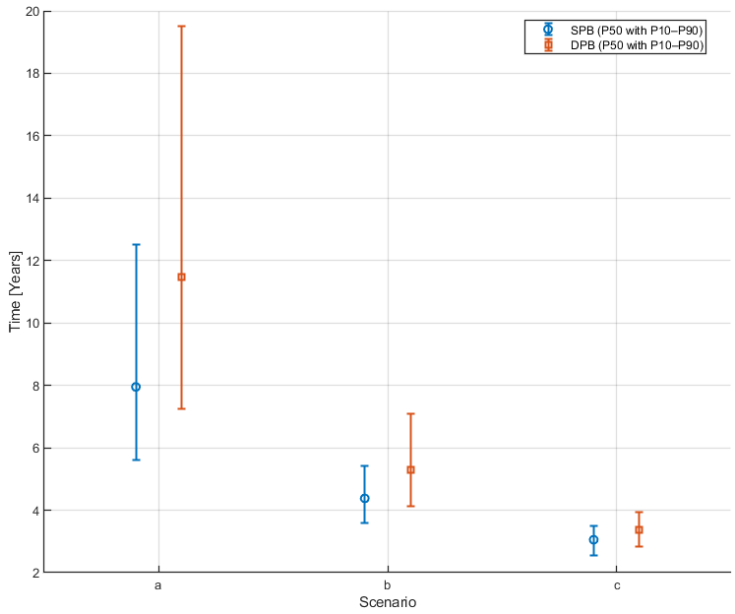

Figure 12. Monte Carlo uncertainty ranges for SPB and DPP across the three fuel-saving scenarios. Markers represent median values (P50) and error bars show the P10-P90 range.

Figures 13(a) and (b) present the Monte Carlo cumulative discounted cashflow over the 25-year project lifetime under the 10.5% and 28.5% case saving, respectively. The solid black line represents the median cumulative net cashflow, while the shaded regions indicate the uncertainty ranges (50%, 80%, and 95% confidence intervals) generated from the simulations.

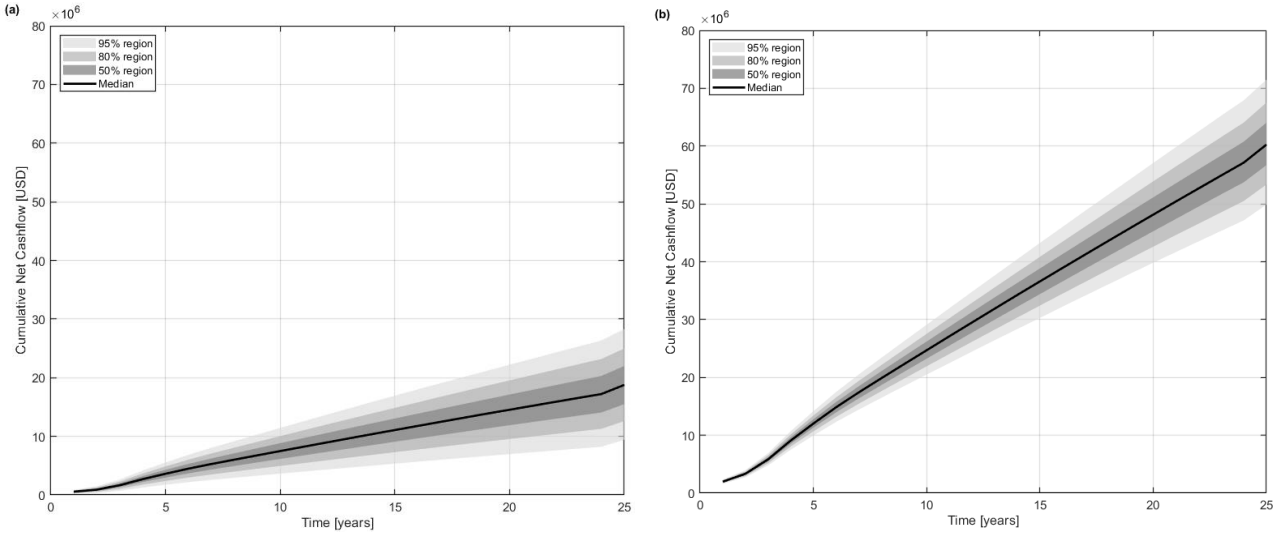

Figure 13. Monte Carlo cumulative discounted cashflow for the 10.5% (a) and 28.5% (b) scenarios, showing the median and uncertainty ranges.

In Figure 13(a), cumulative cashflow increases steadily, reaching ~18-20 MUSD by Year 25. The widening shaded bands show increasing uncertainty over time due to fuel and carbon price variability, but the median trend remains positive, indicating consistent profitability. In Figure 13(b), cumulative cashflow grows faster, reaching ~60 MUSD by Year 25. The steeper slope reflects higher fuel savings and stronger economic performance, while the expanding uncertainty bands still maintain a clearly positive median outcome.

4. CONCLUSIONS

In this work, and integrated framework combining well-to-wake life cycle assessment with an AI-assisted techno-economic model was presented for wind assisted ship propulsion, and applied to the case study of a containership equipped with Flettner rotors. The findings highlights that well-to-tank emissions, often overlooked from regulations, are not negligible. Furthermore, the life cycle of Flettner rotors is primarily driven by emissions during end-of-life and manufacturing. The use of AI for techno-economic assessment, particularly for long term while accounting for uncertainty was also evidenced, with the Random Forest model outperforming the SARIMA one. This work provides novel insights into the use of AI for maritime decarbonisation, and the integration of life cycle assessment for techno-economic assessments, further supporting the environmental and economic viability of wind-assisted ship propulsion. Future work may focus on expanding the current work to a wider parameter space, with additional variables (ship type, ship speed, wind propulsion systems, etc), considerations for application to alternative fuels, increased robustness of the AI forecasting models, and the inclusion of dynamic wind conditions and route strategies to quantify actual savings thanks to wind propulsion instead of the present scenarios for low, medium and high expected savings.

ACKNOWLEDGEMENTS

This work has been funded by the Henderson Innovation Seed Fund (DHV and MF) and the BCU Policy Support Small Grant (JBRGS).

REFERENCES

Admin.ch. (2026). *Das BAFU in Kürze*. Available at: https://www.bafu.admin.ch/de/das-bafu-in-kuerze

Anemoi. (2024). *Anemoi Marine - Rotor Sails for a Sustainable Future*. Available at: https://anemoimarine.com/

Bergmeir, C., and Benítez, J. M. (2012). On the Use of Cross-Validation for Time Series Forecasting. *Information Sciences* 191, pp. 192–213. https://doi.org/10.1016/j.ins.2011.12.028.

Blank, L., and Tarquin, A. (2018). *Engineering Economy*. 8th ed. New York, McGraw-Hill Education. ISBN: 978-0-07-352343-9.

Bouman, E. A., Lindstad, E., Rialland, A. I., and Strømman, A. H. (2017). State-of-the-Art Technologies, Measures, and Potential for Reducing GHG Emissions from Shipping - A Review. *Transportation Research Part D: Transport and Environment* 52, pp. 408–421. https://doi.org/10.1016/j.trd.2017.03.022.

Box, G. E. P., Jenkins, G. M., Reinsel, G. C., and Ljung, G. M. (2015). *Time Series Analysis: Forecasting and Control*. 5th ed. Hoboken, NJ, John Wiley & Sons.

Breiman, L. (2001). Random Forests. *Machine Learning* 45(1), pp. 5–32. https://doi.org/10.1023/A:1010933404324.

Bunker, S. (2019). *Daily Bunker Fuel Prices*. Usda.gov. Available at: https://agtransport.usda.gov/Fuel/Daily-Bunker-Fuel-Prices/4v3x-mj86/about_data

Bureau Veritas (2024). *Wind Propulsion Systems (Rule Note NR206).* Paris: Bureau Veritas Marine & Offshore. Available at: https://erules.veristar.com/dy/data/bv/pdf/206-NR_2025-03.pdf

Carlton, J. (2018). *Marine Propellers and Propulsion*. 4th ed. Oxford: Butterworth-Heinemann (Elsevier).

CE Delft (2016). *Study on the Analysis of Market potentials and Market Barriers for Wind Propulsion Technologies for Ships*. Tech. Rep. CE Delft. Available at: https://cedelft.eu/wp-content/uploads/sites/2/2021/04/CE_Delft_7G92_Wind_Propulsion_Technologies_Final_report.pdf

Chen, Z. S., and Lam, J. S. L. (2022). Life Cycle Assessment of Diesel and Hydrogen Power Systems in Tugboats. *Transportation Research Part D: Transport and Environment,* 103, p.103192. https://doi.org/10.1016/j.trd.2022.103192.

Chou, T., Kosmas, V., Acciaro, M. and Renken, K. (2021). A Comeback of Wind Power in Shipping: An Economic and Operational Review on the Wind-Assisted Ship Propulsion Technology. *Sustainability*, 13(4), pp.1880–1880. https://doi.org/10.3390/su13041880.

Comer, B., Ünalan, S. and Mao, X. (2024). *Updating Marine Engine Emission Standards using Real-World Data: A Potential Update to IMO's NOx Technical Code*. Available at: https://theicct.org/wp-content/uploads/2024/11/ID-222-%E2%80%93-IMO-NOx_brief_final.pdf

Curran, M.A. (2008). Life-Cycle Assessment. *Encyclopedia of Ecology*, pp.2168–2174. doi:https://doi.org/10.1016/b978-008045405-4.00629-7.

Dhainaut, C., Sacher, M., Leroux, J.-B., Pernod, L., and Podeur, V. (2025). *Large-Scale Optimization Framework for Simultaneous Design and Routing of Wind-Assisted Ships*. SNAME Chesapeake Sailing Yacht Symposium. https://doi.org/10.5957/CSYS-2025-014.

DNV (2021). *Maritime Forecast to 2050*. 2021 ed. DNV. Available at: https://dvzpv6x5302g1.cloudfront.net/AcuCustom/Sitename/DAM/114/DNV_Maritime_Forecast_2050_2021.pdf.

Kim, D. M., Hong, S. H., Jeong, S. H. and Kim, S. J. (2024). Analysis of Dynamic Characteristics of Rotor Sail Using a 4DOF Rotor Model and Finite Element Model. *Journal of Marine Science and Engineering*, 12(2), pp.335–335https://doi.org/10.3390/jmse12020335.

European Commission (2023). *Report on CO_2 Emissions from Maritime Transport.* Brussels: European Commission. Available at: https://climate.ec.europa.eu/system/files/2023-03/swd_2023_54_en.pdf

European Maritime Safety Agency (EMSA) (2023). *EMSA Facts and Figures 2023*. Lisbon: European Maritime Safety Agency. Available at: https://www.emsa.europa.eu/damage-stability-study/items.html?cid=77&id=5176

Evergreen-line.com. (2021). *Vessel Type - EVERGREEN LINE*. Available at:

https://www.evergreen-line.com/vesselparticulars/jsp/VSL_VesselType.jsp?vslType=A

Fadaie, S., Thornley, P., & Souppez, J. B. (2025). A Systematic Review of Technologies, Measures, and CO2 Emission Reduction Potential for Maritime Transport Decarbonisation. *Advances in Applied Energy*, 100255. https://doi.org/10.1016/j.adapen.2025.100255

Fisher, I. (1930). *The Theory of Interest*. New York, MacMillan.

Glasserman, P. (2004). *Monte Carlo Methods in Financial Engineering.* New York, Springer. https://doi.org/10.1007/978-0-387-21617-1_1

Ha, S., Jeong, B., Jang, H., Park, C., & Ku, B. (2023). A Framework for Determining the Life Cycle GHG Emissions of Fossil Marine Fuels in Countries Reliant on Imported Energy Through Maritime Transportation: A Case Study of South Korea. *Science of The Total Environment*, 897, 165366. https://doi.org/10.1016/j.scitotenv.2023.165366

Hamilton, S.D., Millstein, D., Bolinger, M., Wiser, R. and Jeong, S. (2020) 'How does wind project performance change with age in the United States?', *Joule,* 4(5), pp. 1004–1020. https://doi.org/10.1016/j.joule.2020.04.005

Hochkirch, K. and Bertram, V. (2022). Wind Assisted Propulsion: Economic and Ecological Considerations. *Maritime Technology and Research*, 4(3). https://doi.org/10.33175/mtr.2022.254498.

Hossein Arabnejad, M., Thies, F., Yao, H.-D. and Ringsberg, J.W. (2025). Life Cycle Assessment Method for Ship Fuels Using a Ship Performance Prediction Model and Actual Operation Conditions - Case Study of Wind-Assisted Cargo Ship. *Energies*, 18(17), p.4559. https://doi.org/10.3390/en18174559.

Huang, J., & Souppez, J. B. (2025). State of the Art in Wind Assisted Ship Propulsion for Maritime Decarbonisation and Sustainable Shipping: A Systematic Review. *Journal of Sailing Technology*, 10(01), 258-278. https://doi.org/10.5957/jst/2025.10.1.258

Hyndman, R. J., and Athanasopoulos, G. (2021). *Forecasting: Principles and Practice*. 3rd ed. Melbourne, OTexts. https://otexts.com/fpp3/

International Maritime Organization (IMO) (2023). *IMO Framework on Life Cycle GHG Intensity of Marine Fuels (LCA).* Available at: https://www.imo.org/en/ourwork/environment/pages/lifecycle-ghg--carbon-intensity-guidelines.aspx

International Maritime Organization (IMO) (2025). *Flettner Rotors: GreenVoyage2050*. Available at: https://greenvoyage2050.imo.org/technology/flettner-rotors/

International Windship Association (IWSA) (2022). *Wind Propulsion Solutions for Commercial Shipping.* Available at: https://wind-ship.org

Investing.com (2023). *Carbon Emissions Futures Historical Data*. Available at: https://uk.investing.com/commodities/carbon-emissions-historical-data

Ipcc.ch. (2023). *AR5 Synthesis Report: Climate Change 2014 - IPCC.* Available at: https://www.ipcc.ch/report/ar5/syr/

Karuppannan Gopalraj, S. and Kärki, T. (2020). A Review on the Recycling of Waste Carbon Fibre/Glass Fibre-Reinforced Composites: Fibre Recovery, Properties and Life-Cycle Analysis. *SN Applied Sciences,* 2(3). https://doi.org/10.1007/s42452-020-2195-4.

Khan, L., Macklin, J., Peck, B., Morton, O., and Souppez, J.-B. R. G. (2021). *A Review of Wind-Assisted Ship Propulsion for Sustainable Commercial Shipping: Latest Developments and Future Stakes*. Wind Propulsion Conference. Royal Institution of Naval Architects.

Kolodziejski, M. and Sosnowski, M. (2025). Review of Wind-Assisted Propulsion Systems in Maritime Transport. *Energies*, 18(4). https://doi.org/10.3390/en18040897

Kramel, D., Muri, H., Kim, Y. R., Lonka, R., Nielsen, J. B., Ringvold, A. L., Bouman, E. A., Steen, S., and Strømman, A. H. (2021). Global shipping emissions from a well-to-wake perspective: The MariTEAM model. *Environmental Science & Technology.* https://doi.org/10.1021/acs.est.2c01301 .

Kroese, D. P., Taimre, T., and Botev, Z. I. (2011). *Handbook of Monte Carlo Methods*. Chichester, John Wiley & Sons. https://doi.org/10.1002/9781118014967

Lan, T., Huang, L., Ruan, Z., Cao, J., Ma, R., Wu, J., ... & Wang, K. (2025). Multilevel Parallel Integration Framework for Enhancing Energy Efficiency of Wing-Assisted Ships Based on Deep Learning and Intelligent Algorithms: Towards A Smarter and Greener Shipping. *Applied Energy*, 394, 126202. https://doi.org/10.1016/j.apenergy.2025.126202

Laursen, R., Patel, H., Sofiadi, D., Zhu, R., Nelissen, D., Van Seters, D., Pang, E., 2023. *Potential of Wind-Assisted Propulsion for Shipping.* European Maritime Safety Agency (EMSA) Report (EMSA/OP/43/2020), 1–271.

Li, D., Ma, R., Zhao, Q., Zhao, H., Ruan, Z., Wang, T., ... & Huang, L. (2025). A Novel Deep Reinforcement Learning Based Joint Optimization Method of Wind-Assisted Ship Energy Efficiency Considering Dynamic Environmental Factors. *Ocean Engineering*, 339, 122085. https://doi.org/10.1016/j.oceaneng.2025.122085

Lindstad, E., Eskeland, G. S., Rialland, A., and Valland, A. (2020). Decarbonizing Maritime Transport: The Importance of Engine Technology and Regulations for LNG to Serve as a Transition Fuel. *Sustainability* 12(21), 8793. https://doi.org/10.3390/su12218793.

Mavroudis (2021). *World's Largest Container Ship Called at Hamburg*. Mavroudis.com.cy. Available at: https://www.mavroudis.com.cy/news/worlds-largest-container-ship-called-at-hamburg

MyDello (2024) *Suez Canal Shipping Guide*. Available at: https://mydello.com/suez-canal-shipping/

Nguyen, S., Gadel, M., Wang, K., Li, J., Zhang, X., Kong, S. C., ... & Qin, Z. (2025). Maritime Decarbonization Through Machine Learning: A Critical Systematic Review of Fuel and Power Prediction models. *Cleaner Logistics and Supply Chain*, 14, 100210. https://doi.org/10.1016/j.clscn.2025.100210

Norsepower (2022). *Norsepower Rotor Sail™ Case Studies and Performance Data*. Norsepower Oy Ltd. ULR: https://www.norsepower.com/app/uploads/2025/04/Norsepower-Brochure-91-Screen-version.pdf

Openlca.org. (2026). *openLCA Nexus: The Source for LCA Data Sets.* Available at: https://nexus.openlca.org/database/BAFU

Pachauri, R., Meyer, L., Hallegatte, S., Hegerl, G., Van Ypersele, J.-P., Brinkman, S., Leprince-Ringuet, N. and Van Boxmeer, F. (2014). *Climate Change 2014 Synthesis Report*. IPCC. Gian-Kasper Plattner. Available at: https://www.ipcc.ch/site/assets/uploads/2018/02/SYR_AR5_FINAL_full.pdf.

Pedregosa, F., Varoquaux, G., Gramfort, A., Michel, V., Thirion, B., Grisel, O., Blondel, M., Prettenhofer, P., Weiss, R., Dubourg, V., Vanderplas, J., Passos, A., Cournapeau, D., Brucher, M., Perrot, M., and Duchesnay, É. (2011). Scikit-Learn: Machine Learning in Python. *Journal of Machine Learning Research* 12, pp. 2825–2830. https://jmlr.org/papers/v12/pedregosa11a.html.

Port of Hamburg (2024). *Ever Ace - Ship Specials.* Available at: https://www.hafen-hamburg.de/en/all-vessels/ship-specials/ever-ace/

Reche-Vilanova, M. (2025). *Wind Propulsion Systems For Commercial Ships: Modelling, Design and Economic Optimisation*. PhD Thesis, Technical University of Denmark.

Reche-Vilanova, M., Bingham, H. B., Fluck, M., Morris, D., & Psaraftis, H. N. (2025). Cost–Benefit Analysis and Design Optimization of Wind Propulsion Systems for a Tanker Retrofit Case. *Maritime Transport Research,* 8, 100132. https://doi.org/10.1016/j.martra.2025.100132

Roux, M., Lodato, C., Laurent, A., & Astrup, T. F. (2024). A Review of Life Cycle Assessment Studies of Maritime Fuels: Critical Insights, Gaps, And Recommendations. *Sustainable Production and Consumption,* 50, 69-86. https://doi.org/10.1016/j.spc.2024.07.016

SeaRates. (2026). Distance & Transit Time Calculator - SeaRates. Available at: https://www.searates.com/distance-time/

Ship-Technology (2023) *Mega Container Ships and How They Are Changing Ports.* Available at: https://www.ship-technology.com/features/featuremega-container-ships-and-how-they-are-changing-ports/

Styhre, L., Winnes, H., Black, J., Lee, J. and Le-Griffin, H. (2017). Greenhouse Gas Emissions from Ships in Ports – Case Studies in Four Continents. *Transportation Research Part D: Transport and Environment,* 54, pp.212–224. https://doi.org/10.1016/j.trd.2017.04.033

Suez Canal Authority (n.d.) Frequently Asked Questions. Available at: https://www.suezcanal.gov.eg/English/Pages/FAQ.aspx

Talluri, L., Nalianda, D.K., Kyprianidis, K.G., Nikolaidis, T. and Pilidis, P. (2016). Techno Economic and Environmental Assessment of Wind Assisted Marine Propulsion Systems. *Ocean Engineering*, 121, pp.301–311. https://doi.org/10.1016/j.oceaneng.2016.05.047.

Tillig, F., Ringsberg, J.W., Psaraftis, H.N. and Thalis Zis (2020). Reduced Environmental Impact of Marine Transport Through Speed Reduction and Wind Assisted Propulsion. *Transportation Research Part D Transport and Environment,* 83, pp.102380–102380. https://doi.org/10.1016/j.trd.2020.102380.

Travelinho (2022). *What is the Carbon Footprint of Sea Freight and Ferries*? Medium. Available at: https://medium.com/@travelinho/carbon-footprint-sea-transport-98f97d42852f

UNCTAD (2023) Container Ports: Fastest, Busiest and Best Connected. Available at: https://unctad.org/news/container-ports-fastest-busiest-and-best-connected

United States Department of Agriculture (USDA) (n.d.). *Daily Bunker Fuel Prices*. Daily Bunker Fuel Prices | Open Ag Transport Data

U.S. Energy Information Administration (2025). *International Energy Statistics and Fuel Price Data.* Available at: https://www.eia.gov

Watari, T., Fishman, T., Wieland, H. and Wiedenhofer, D. (2025). Global Stagnation and Regional Variations in Steel Recycling. *Resources, Conservation and Recycling*, 220, p.108363. https://doi.org/10.1016/j.resconrec.2025.108363.

Weron, R. (2014). Electricity Price Forecasting: A Review of the State-Of-The-Art with a Look into the Future. *International Journal of Forecasting* 30(4), pp. 1030–1081. https://doi.org/10.1016/j.ijforecast.2014.08.008.

Wingd.com. (2026). *X92-B.* Available at: https://wingd.com/products-solutions/engines/x92-b

Zamboni, G., Scamardella, F., Gualeni, P., & Canepa, E. (2024). Comparative Analysis Among Different Alternative Fuels for Ship Propulsion in a Well-To-Wake Perspective. *Heliyon*, 10(4). https://doi.org/10.1016/j.heliyon.2024.e26016

Zhang, Y., Fung, J.C.H., Chan, J.W.M. and Lau, A.K.H. (2019). The Significance of Incorporating Unidentified Vessels into AIS-Based Ship Emission Inventory. *Atmospheric Environment*, 203, pp.102–113. https://doi.org/10.1016/j.atmosenv.2018.12.055

Zhang, Y., Chang, Y., Wang, C., Fung, J.C.H. and Lau, A.K.H. (2022). Life-Cycle Energy and Environmental Emissions of Cargo Ships. *Journal of Industrial Ecology*, 26(6), pp.2057–2068. https://doi.org/10.1111/jiec.13293.

Zou, J. and Yang, B. (2023). Evaluation Of Alternative Marine Fuels from Dual Perspectives Considering Multiple Vessel Sizes. *Transportation Research Part D: Transport and Environment*, 115, p.103583. https://doi.org/10.1016/j.trd.2022.103583